

See discussions, stats, and author profiles for this publication at: <https://www.researchgate.net/publication/11190129>

Synthesis, Structure, and Biological Evaluation of Novel N – and O –Linked Diinositols

ARTICLE *in* JOURNAL OF THE AMERICAN CHEMICAL SOCIETY · OCTOBER 2002

Impact Factor: 12.11 · DOI: 10.1021/ja0205378 · Source: PubMed

CITATIONS

45

READS

21

6 AUTHORS, INCLUDING:



Ion Ghiviriga

University of Florida

184 PUBLICATIONS **2,551** CITATIONS

SEE PROFILE



Khalil Abboud

University of Florida

582 PUBLICATIONS **12,667** CITATIONS

SEE PROFILE

Synthesis, Structure, and Biological Evaluation of Novel *N*- and *O*-Linked Diinositols

Bernhard J. Paul, Jerremey Willis, Theodore A. Martinot, Ion Ghiviriga,[†]
Khalil A. Abboud,[‡] and Tomas Hudlicky*

Contribution from the University of Florida, Department of Chemistry, PO Box 117200,
Gainesville, Florida 32611

Received April 15, 2002

Abstract: Several *O*- and *N*-linked inositols and/or aminoinositols have been prepared by iterative opening of epoxides and aziridines derived from homochiral cyclohexadiene *cis*-diols. The three inositols and their intermediate conduritols (conduramines) were tested against several glycosidases (α - and β -glucosidase, α - and β -galactosidase, α - and β -mannosidase) in an assay that measured the rate of hydrolysis of *p*-nitrophenolglycosides rather than the concentration of *p*-nitrophenolate. Somewhat surprisingly, the best inhibition was seen against β -galactosidase with several of the compounds. The inositols linked through oxygen or nitrogen were subjected to calcium binding studies performed in NMR experiments. Detailed analysis of the title compounds by NMR spectroscopy has been performed, and full assignments were made. One of the attendant benefits of the preparation of these compounds has been expressed in the design and synthesis of new salen catalysts whose effectiveness has been compared with Jacobsen's catalyst in the epoxidation of styrene.

Introduction

Investigations of the biological function of sugars have witnessed enormous progress over the last several years, and cellular processes such as recognition events are now more understood, allowing for the development of carbohydrate-based drugs.¹ Unnatural derivatives of carbohydrates have been at the forefront of bioorganic chemistry research primarily because of their ability to mimic the structure of monosaccharides and hence serve as inhibitors of glycosidases. Since these enzymes are involved in a variety of different biological processes, such research naturally leads to potential applications in the treatment of diabetes,² viral infections,³ and cancer.³

Recent literature presents many examples of simple carbohydrates in which the oxygen has been replaced with carbon (pseudosugars),⁴ nitrogen (iminosugars),^{5,6} sulfur,⁷ and other

atoms or groups.⁸ Along with polyhydroxylated alkaloids,⁹ most such derivatives show modest to excellent inhibition of the common glycosidases that would be involved in the initial steps of cell penetration by the viral material. Similarly, disaccharides and even oligosaccharides have been modified¹⁰ and studied further for their role in the inhibition of glycosidases.

Several years ago we disclosed the preparation of a series of simple oligomers containing the configuration of *L-chiro*-inositol as shown by the general structure **1**, Figure 1.¹¹ The initial reason for investigating such compounds was based on the assumption that *O*-linked oligomers of this type may play a role in insulin mediation¹² and at the same time not be sensitive to the gastric environment, thus being potential candidates for orally administered medicines.

A number of oligomers have been prepared,¹³ and some of these compounds proved to have interesting metal chelating properties¹⁴ and displayed tertiary structures in solid state. In an effort to investigate compounds that would mimic the

* Address correspondence to this author. E-mail: hudlicky@chem.ufl.edu.

[†] To whom correspondence regarding NMR spectroscopy should be addressed.

[‡] To whom correspondence regarding X-ray crystallography should be addressed.

- (1) (a) Dwek, R. A. *Chem. Rev.* **1996**, 96, 683–720. (b) Yarema, K. J.; Bertozzi, C. R. *Curr. Opin. Chem. Biol.* **1998**, 2, 49–61. (c) Sears, P.; Wong, C.-H. *Angew. Chem., Int. Ed.* **1999**, 38, 2300–2324. (d) Alper, J. *Science* **2001**, 291, 2338–2343. (e) Gruner, S. A. W.; Locardi, E.; Lohof, E.; Kessler, H. *Chem. Rev.* **2002**, 102, 491–514.
- (2) Truscheit, E.; Hillebrand, I.; Junge, B.; Müller, L.; Puls, W.; Schmid, D. *Prog. Clin. Biochem. Med.* **1988**, 7, 17–99.
- (3) Zitzmann, N.; Mehta, A. S.; Carrouee, S.; Butters, T. D.; Platt, F. M.; McCauley, J.; Blumberg, B. S.; Dwek, R. A.; Block, T. M. *Proc. Natl. Acad. Sci.* **1999**, 96, 11878–11882.
- (4) Ferrier, R. J.; Middleton, S. *Chem. Rev.* **1993**, 93, 2779–2831.
- (5) Stuetz, A. E. *Iminosugars as Glycosidase Inhibitors*; Wiley-VCH: Weinheim, 1998.
- (6) Berecibar, A.; Grandjean, C.; Siriwardena, A. *Chem. Rev.* **1999**, 99, 779–844.
- (7) Robina, I.; Vogel, P.; Witczak, Z. J. *Curr. Org. Chem.* **2001**, 5, 1177–1214.

- (8) Lillelund, V. H.; Jensen, H. H.; Liang, X.; Bols, M. *Chem. Rev.* **2002**, 102, 515–553.
- (9) (a) Asano, N.; Nash, R. J.; Molyneux, R. J.; Fleet, G. W. J. *Tetrahedron: Asymmetry* **2000**, 11, 1645–1680. (b) Watson, A. A.; Fleet, G. W. J.; Asano, N.; Molyneux, R. J.; Nash, R. J. *Phytochemistry* **2001**, 56, 265–295.
- (10) Liu, L.; McKee, M.; Postema, M. H. D. *Curr. Org. Chem.* **2001**, 5, 1133–1167.
- (11) Paul, B. J.; Martinot, T. A.; Willis, J.; Hudlicky, T. *Synthesis* **2001**, 952–956.
- (12) (a) Ley, S. V.; Yeung, L. L. *Synlett* **1992**, 997–998. (b) Reddy, K. K.; Falck, J. R.; Capdevila, J. *Tetrahedron Lett.* **1993**, 34, 7869–7872.
- (13) (a) Hudlicky, T.; Abboud, K. A.; Entwistle, D. A.; Fan, R.; Maurya, R.; Thorpe, A. J.; Bolonick, J.; Myers, B. *Synthesis* **1996**, 897–911. (b) Desjardins, M.; Lallemant, M.-C.; Hudlicky, T.; Abboud, K. A. *Synlett* **1997**, 728–730. (c) Desjardins, M.; Lallemant, M.-C.; Freeman, S.; Hudlicky, T.; Abboud, K. A. *J. Chem. Soc., Perkin Trans. 1* **1999**, 621–628.
- (14) Hudlicky, T.; Abboud, K. A.; Bolonick, J.; Maurya, R.; Stanton, M. L.; Thorpe, A. J. *J. Chem. Soc., Chem. Commun.* **1996**, 1717–1718.

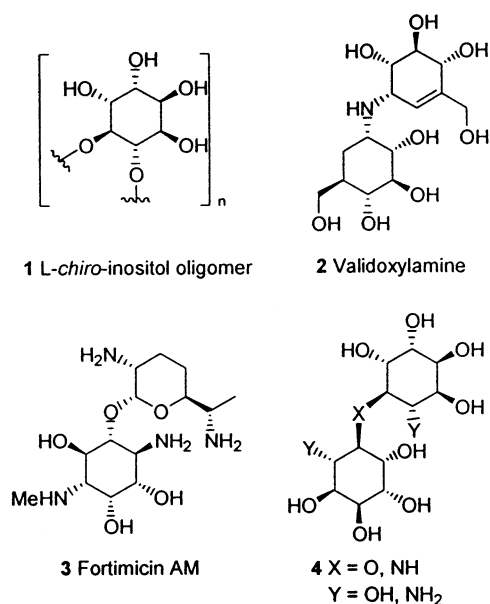


Figure 1. Structural comparison of *N*- and *O*-linked (amino)inositol oligomers to natural occurring antibiotics.

connectivity found in naturally occurring antibiotics such as validoxylamine **2** and fortimicin **3**, Figure 1,¹⁵ we wished to prepare and examine *O*- and *N*-linked oligomers that would contain such a motif. To this end, *N*- and *O*-linked diinositols and their precursory conduritols (or conduramines) would be targeted in order that their biological properties may be examined against common glycosidases. In this article we report the details of the syntheses of compounds of the general type **4**, the preparation of some of which has been disclosed in a preliminary form and which lend themselves to further oligomerizations through the interaction of Y with either epoxides or aziridines.¹¹ In addition, the results of testing of these compounds against six glycosidases are provided. The future potential of these compounds as three-dimensional templates for transfer of C–O chiral connectivity to C–C asymmetry is also indicated.

Synthesis

Bromocyclohexadiene-*cis*-diol (**5**)¹⁶ was obtained by whole-cell fermentation of bromobenzene with *E. coli* JM109(pDTG601), an organism that expresses toluene dioxygenase (TDO) and was further converted to vinyl epoxide **6**.¹⁷ Reaction of **6** with ammonia in the presence of Yb(OTf)₃ resulted in rapid ring opening of the epoxide to give an amino alcohol as the intermediate product, which was without isolation treated with another equivalent of vinyl epoxide **6** to afford dimer **7** in a one-pot process in 78% yield, Scheme 1. Removal of the bromine atoms under radical conditions (AIBN, Bu₃SnH) afforded alkene **8** in 83% yield. Treatment of **8** with HCl in MeOH yielded amine-linked diconduritol **9** as its hydrochloride (84%).

Acylation of **8** with acetic anhydride under rather vigorous conditions afforded acetamide **10** (88%). Hydrolysis of the ester groups in **10** under basic conditions (NaOMe, MeOH) followed by acidic cleavage of the acetonides (TFA/THF/H₂O) provided the acetamide-linked diconduritol **11** in 85% yield for two steps.

To obtain the fully hydroxylated species, dimer **10** was subjected to OsO₄-catalyzed dihydroxylation (OsO₄ cat./NMNO/acetone/H₂O) followed by protection of the resulting diols as their acetonides (DMP, H⁺) to give dimer **12** in 60% yield for two steps. Hydrolysis of the esters (NaOMe, MeOH) followed by removal of the acetonides under acidic conditions (HCl, MeOH) furnished the acetamide-linked diinositol **13** in 57% yield (two steps).

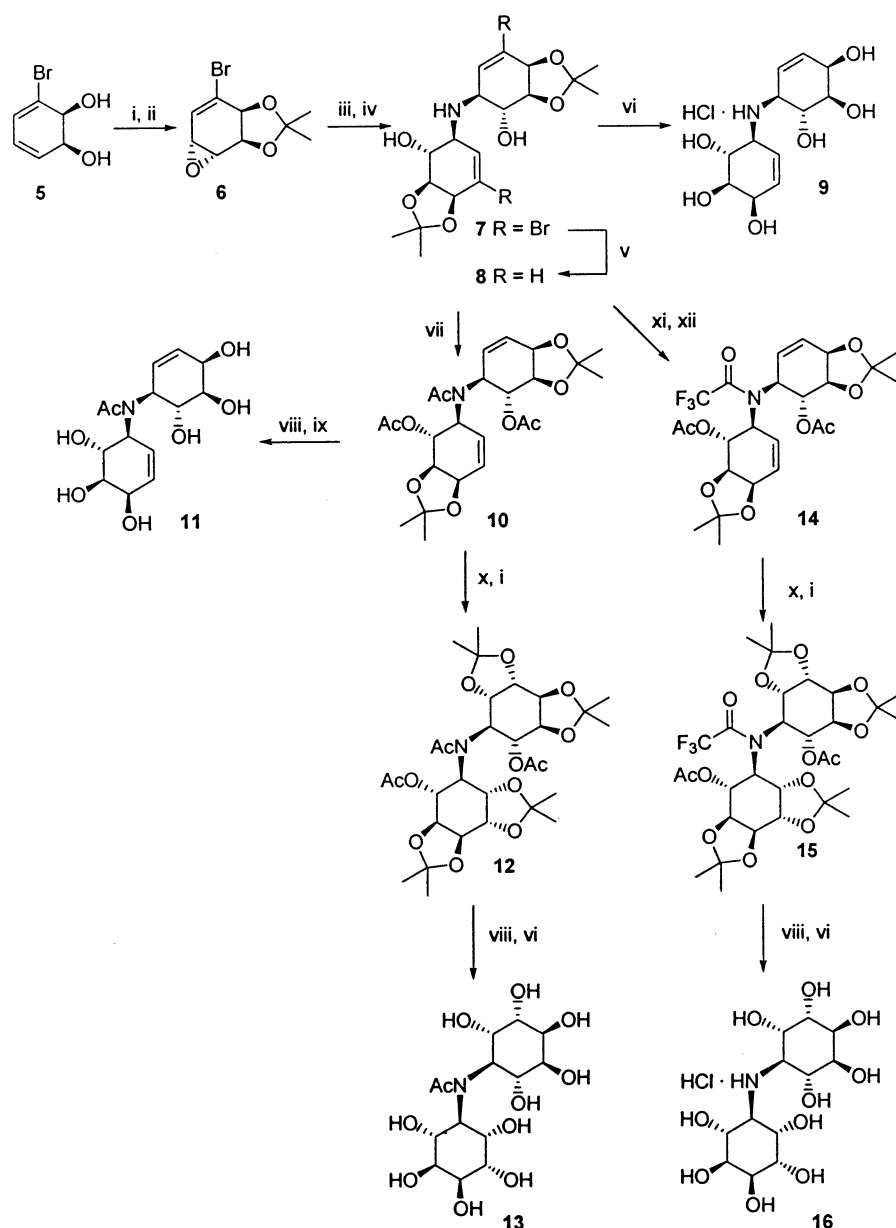
For the synthesis of amine-linked diinositol **16**, compound **8** was treated with acetic anhydride at low temperature to achieve acylation of the alcohols only, leaving the sterically hindered secondary amine untouched. Acylation of the latter with trifluoroacetic anhydride provided trifluoroacetamide **14** (78% for two steps). Oxidation with a catalytic amount of OsO₄ followed by protection of the resulting diols as their acetonides gave the fully hydroxylated species **15** (53%). Cleavage of the esters as well as the trifluoroacetamide under basic conditions (NaOMe, MeOH) followed by acidic hydrolysis (HCl, MeOH) provided amine-linked diinositol **16** as its hydrochloride in 75% yield. For the synthesis of diaminoinositol dimer **17**, diol **5** was converted to vinyl aziridine **18** according to a known procedure.^{17,18} Ring opening of **18** was achieved with ammonia under Yb(OTf)₃ catalysis followed by treatment of the intermediate amine with another equivalent of vinyl epoxide **6** to afford amine **19** in 78–94% yield. Conversion of the alcohol into its acetate provided amine **20** (93%), which was subsequently converted to trifluoroacetamide **21** (92–98%). Removal of the halogens under radical conditions (AIBN, Bu₃SnH) afforded alkene **22** in 56–73% yield. Osmylation of the double bonds followed by protection of the resulting diols as their acetonides afforded the fully oxygenated species **23** in 26–61% yield. Hydrolysis of the acetate and trifluoroacetamide under basic conditions (57%), removal of the sulfonamide with Na in liquid ammonia (84%), and acidic hydrolysis of the acetonides afforded diinositol **17** as its hydrochloride salt in 77% yield. For the preparation of oxygen-linked diinositol **24**, we envisioned a convergent strategy. Vinyl epoxide **6** was opened under basic conditions to provide diol **25** in 63% yield. Reaction of **25** with vinyl aziridine **18** under BF₃·Et₂O catalysis afforded a mixture of two ethers **26a** (52%) and **26b** (18%), along with several byproducts (vide infra). Removal of the halogens under radical conditions gave **27a** (92%) and **27b** (86%). After hydroxylation of the double bonds and protection of the resulting diols as acetonides, both isomers converged into a single compound **28** (65%). Deprotection of the tosylamide with Na in liquid ammonia followed by hydrolysis of the acetals under acidic conditions provided free dimer **24** as its hydrochloride salt in 52% yield.

Upon examining the byproducts of the Lewis-acid-mediated coupling, we were also able to identify compounds **26c**, **29**, and **30** in the reaction mixture (Figure 2).

The presence of the *cis*-configured dimer **26c** was somewhat surprising and indicated that this material was formed by an

- (15) (a) Ogawa, S.; Ogawa, T.; Chida, N.; Toyokuni, T.; Suami, T. *Chem. Lett.* **1982**, 749–752. (b) Ogawa, S.; Ogawa, T.; Iwasawa, Y.; Toyokuni, T.; Chida, N.; Suami, T. *J. Org. Chem.* **1984**, 49, 2594–2599.
- (16) (a) Gibson, D. T.; Hensley, M.; Yoshioka, H.; Mabry, T. J. *Biochemistry* **1970**, 9, 1626–1630. (b) Hudlicky, T.; Luna, H.; Barbieri, G. L.; Kwart, L. D. *J. Am. Chem. Soc.* **1988**, 110, 4735–4741. (c) Hudlicky, T.; Stabile, M. R.; Gibson, D. T.; Whited, G. M. *Org. Synth.* **1999**, 76, 77–85.
- (17) Hudlicky, T.; Tian, X. R.; Königsberger, K.; Rouden, J. *J. Org. Chem.* **1994**, 59, 4037–4039.

- (18) (a) Tian, X. R.; Hudlicky, T.; Königsberger, K. *J. Am. Chem. Soc.* **1995**, 117, 3643–3644. (b) Hudlicky, T.; Tian, X. R.; Königsberger, K.; Maurya, R.; Rouden, J.; Fan, B. *J. Am. Chem. Soc.* **1996**, 118, 10752–10765.

Scheme 1^a

^a Reagents and conditions: (i) DMP, H⁺; (ii) *m*CPBA, CH₂Cl₂; (iii) NH₃, Yb(OTf)₃; (iv) **6**, dioxane, Δ; (v) AIBN, Bu₃SnH, THF; (vi) HCl, MeOH; (vii) Ac₂O, pyr. DMAP, dioxane, Δ; (viii) NaOMe, MeOH; (ix) THF, TFA, H₂O (2:2:1); (x) OsO₄, NMNO, acetone, H₂O; (xi) Ac₂O, pyr. DMAP, CH₂Cl₂, 0 °C; (xii) TFAA, pyr. DMAP, dioxane Δ.

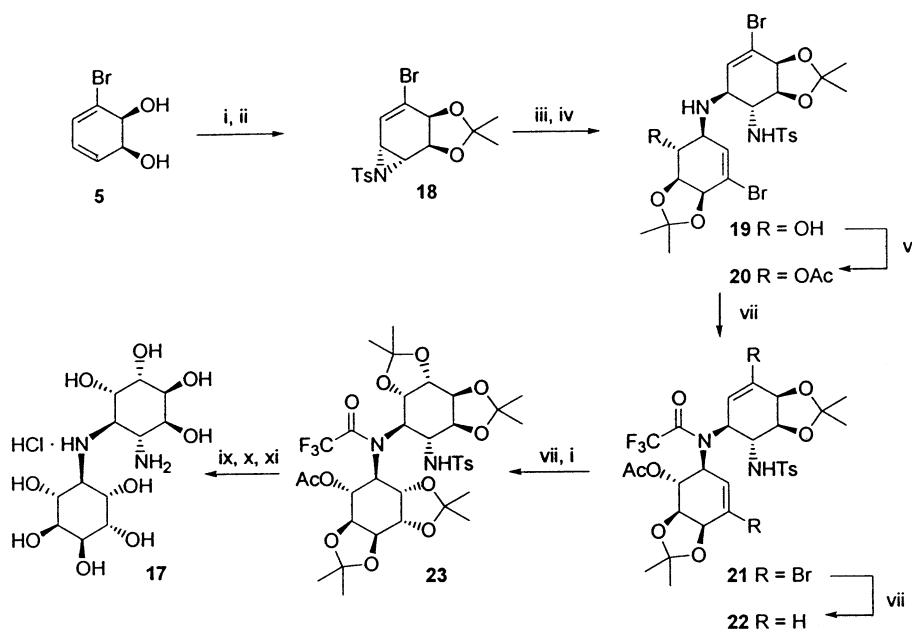
S_N1-type mechanism. Surprisingly, the relative ratio of these products (**26a**:**26b**:**26c**:**29**:**30** = 2:1:1:1:1) proved to be generally unaffected by changes in temperature, catalyst concentration, and solvent, except for a higher percentage of **30** in the reaction mixture at high catalyst concentrations.

Structure Assignment by NMR

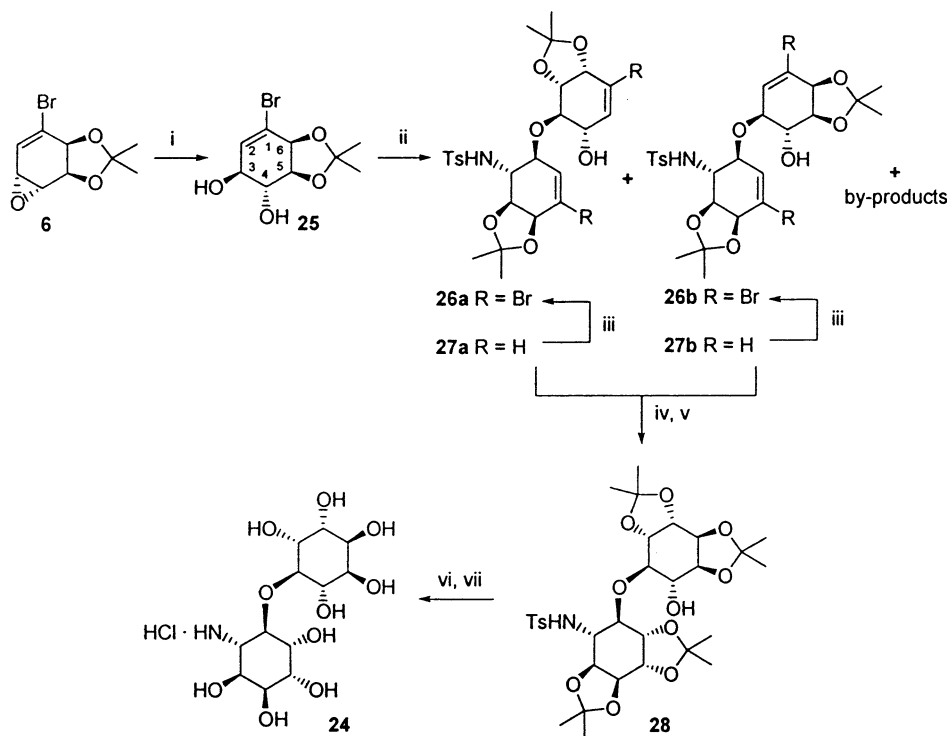
The structure assignments of the *N*- and *O*-linked oligomers were inferred initially from first principles of reactivity of epoxides and aziridines (assuming *trans*-diaxial opening of the strained three-membered rings with nucleophiles) and confirmed by detailed analysis of ¹H NMR spectra and, in some cases, by X-ray crystallography.

Severe overlap of the ring protons in the dimers having different inositol moieties prevented the assignment of the proton signals; however they displayed the expected 10 H(C)–H(X)

pairs in the DQCOSY spectra recorded in DMSO-*d*₆. For dimers **16** and **16a**, having identical inositol units, complete ¹H and ¹³C assignments were made on the basis of the ¹H–¹H and ¹H–¹³C correlations seen in the GHMQC, GHMBC, DQCOSY, and NOESY spectra. The size of the coupling constants between the CH protons in positions 1 through 6 confirmed the stereochemistry of the inositol rings. The chemical shifts in DMSO-*d*₆ at 25 °C were referenced to TMS and are given in Table 1. Variable-temperature spectra in the interval 25–75 °C afforded the temperature coefficients of the ¹H chemical shifts, also reported in Table 1. The relative exchange rates of the OH protons with water, measured in the NOESY spectrum, paralleled the temperature coefficients, indicating that the latter are indicative of the accessibility of the OH groups to the solvent molecules. The NOEs are not very useful in the study of the conformation in solution of these molecules because of their

Scheme 2^a

^a Reagents and conditions: (i) DMP, H⁺; (ii) PhINTs, Cu(acac)₂, CH₃CN; (iii) NH₃, Yb(OTf)₃, (iv) **6**, dioxane, Δ; (v) Ac₂O, pyr. DMAP, CH₂Cl₂; (vi) TFAA, pyr. DMAP, Δ; (vii) AIBN, Bu₃SnH, THF, (viii) OsO₄, NMNO, acetone, H₂O; (ix) NaOMe, MeOH; (x) Na, NH₃ (l); (xi) HCl, MeOH.

Scheme 3^a

^a Reagents and conditions: (i) KOH, DMSO, Δ; (ii) BF₃·Et₂O, **18**; (iii) AIBN, Bu₃SnH, THF; (iv) OsO₄, NMNO, acetone, H₂O; (v) DMP, H⁺; (vi) Na, NH₃ (l); (vii) HCl, MeOH.

symmetry. The NOESY spectrum of **16**, however, revealed fast exchange between the NH₂⁺ protons at 8.10 ppm and the OH protons in position 4, at 5.55 ppm. Corroborating this with a small temperature coefficient for the OH in position 2 (5.24 ppm), indicative of intramolecular hydrogen bonding, one can infer for **16** a solution conformation in which rotation about the C–N bonds brings the OH's in position 2 closer, within a distance appropriate for mutual hydrogen bonding, and the OH's in position 6 closer to the ammonium protons.

The NMR data for compounds **26a–c** raises intriguing questions about the outcome of the ring opening of aziridine **18** by diol **25**. Both the ¹H–¹H vicinal couplings and the ¹H–¹³C long-range couplings confirm that **26b** results from the reaction of the hydroxyl at C-3 of diol **25**, while **26a** and **26c** are the products of the reaction of the C-4 hydroxyl in **25**. The values of the coupling constants given in Figure 1 demonstrate that **26a** and **26b** are indeed the expected products of *trans* aziridine ring opening, but in **26c** strongly support a structure

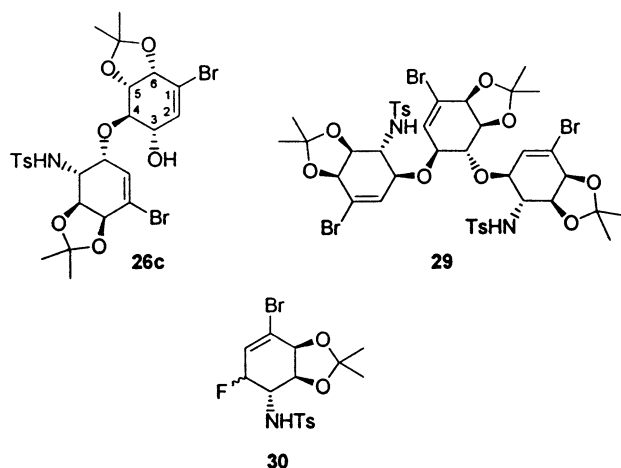


Figure 2. Byproducts of the $\text{BF}_3 \cdot \text{Et}_2\text{O}$ -catalyzed coupling reaction.

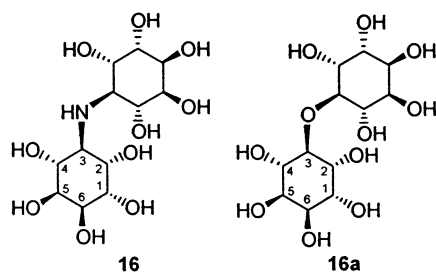


Figure 3. Position numbering for compounds **16** and **16a**.

Table 1. ^1H and ^{13}C Chemical Shifts and Temperature Coefficients of the ^1H Chemical Shifts for Compounds **16** and **16a**

position	16				16a			
	δ_{HCH} (ppm)	δ_{C} (ppm)	δ_{HOH} (ppm)	$d\delta_{\text{HOH}}/dT$ (ppb/K)	δ_{HCH} (ppm)	δ_{C} (ppm)	δ_{H} (ppm)	$d\delta_{\text{HOH}}/dT$ (ppb/K)
1	3.72	72.5	5.2	−4.8	3.72	72.4	4.49	−6.7
2	3.95	68.1	5.24	−1.6	3.65	71.9	5.68	−4.2
3	3.53	63.7			3.43	65.7		
4	3.75	70.1	5.55	−4.4	3.47	73.8	5.62	−6
5	3.49	71.5	4.77	−6.4	3.5	71.6	4.16	−7.6
6	3.68	72.2	4.96	−5.2	3.67	72.7	4.46	−5.4

in which the ring opening occurred *cis*, indicative of an $\text{S}_{\text{N}}1$ -like substitution of a cation or its ion pair.

The chemical shifts given in Table 1 have been determined in CDCl_3 at 25 °C. The chemical shift assignment was based on ^1H – ^1H couplings seen in selective decoupling experiments, and on one-bond and long-range ^1H – ^{13}C couplings seen in GHMQC and GHMBC spectra, respectively.

The assignment of methyls of the acetonide groups was made based on the NOEs seen in the NOESY spectra, namely, strong NOEs between H8 and H5, H6 and between H7' and H5', H6'. The temperature coefficients of the chemical shifts have been measured in CDCl_3 , in the temperature interval −25 to 55 °C. The consistency of the coupling constants $^3J_{\text{H4-H5}}$, $^3J_{\text{H4'-H5'}}$, $^3J_{\text{H5-H6}}$, and $^3J_{\text{H5'-H6'}}$ in compounds **26a–c** clearly demonstrates that both cyclohexene rings in all three compounds are in the same conformation, one in which the hydrogens in positions 4, 5, 4', 5' are pseudoaxial. Vicinal coupling constants of 8–9 Hz for the protons in positions 3', 4', and 5' in compounds **26a–c** confirm that these protons are all pseudoaxial. A value of ca. 2 Hz for $^3J_{\text{H2'-H3'}}$ also indicates that H3' is axial, a position in which the dihedral angle H2'–C2'–C3'–H3' is close to 90°. The similarity of the vicinal coupling constants on the ring

Table 2. ^1H and ^{13}C Chemical Shifts and Temperature Coefficients of the ^1H Chemical Shifts for Compounds **26a–c**

position	26a			26b			26c		
	δ_{H} (ppm)	$d\delta_{\text{H}}/dT$ (ppb/K)	δ_{C} (ppm)	δ_{H} (ppm)	$d\delta_{\text{H}}/dT$ (ppb/K)	δ_{C} (ppm)	δ_{H} (ppm)	$d\delta_{\text{H}}/dT$ (ppb/K)	δ_{C} (ppm)
1			120			120.4			122.7
2	6.36	0	133.6	6.37	0.4	133.2	6.47	−0.3	132.2
3	4.15	0	77.7	3.96	2	77.5	3.92	9.7	76.2
4	3.67	0.5	57.2	3.62	0	56.7	3.53	2.3	55
5	4.07	0.5	77.1	4.15	0.4	76	4.3	−0.7	74.8
6	4.61	−0.5	77.2	4.61	0.1	77.3	4.63	−1.2	77.4
7	1.43	−0.1	27.8	1.41	0.7	27.9	1.33	−2.7	27.7
8	1.33	−0.2	26.2	1.34	0.6	26.4	1.36	−1.2	26.2
9			111.4			118.8			110.5
1'			119.2			118.4			117.8
2'	6.22	−0.1	134.3	5.98	3.4	132.7	6.26	−1.7	135.9
3'	3.97	0.5	69.3	3.8	0.9	78.3	4.12	−1.7	70.5
4'	3.44	0.8	81.4	3.48	2.7	72.7	3.18	6	83.8
5'	4.17	1.9	77.4	4.04	−0.1	77.3	4.03	1.3	77.4
6'	4.63	0.1	77.4	4.62	−0.7	77.2	4.61	−0.2	77.6
7'	1.43	0	25.9	1.57	0.4	28.4	1.39	2.7	26
8'	1.54	0	28	1.42	−0.1	26	1.39	−0.2	27.6
9'			111.2			111.4			111
OH	2.76	−5.2		2.6	−4.1		4.01	−19.3	
NH	5.34	−6.5		4.76	−11		6.58	−19.8	
1''			139.1			138			137.8
2''	7.83	0.2	127.7	7.78	0.6	127.4	7.84	−0.8	127.7
3''	7.29	−0.2	129.4	7.3	0	129.9	7.32	−0.8	129.9
4''	–	–	143.3			144			144.1
5''	2.42	0	21.7	2.44	0	22.2	2.42	−0.3	21.4

originating in aziridine of **26b** to the coupling constants on the rings originating in diol of **26a–c** demonstrates that **26b** is the product of *trans* ring opening (with H3, H4, and H5 all pseudoaxial) and that the coupling constants do not depend significantly on the substitution pattern of the ring. The values of the vicinal coupling constants of H3 in **26c**, $^3J_{\text{H2-H3}} = 5.5$ Hz and $^3J_{\text{H3-H4}} = 3.7$ Hz, clearly demonstrate that this hydrogen is equatorial and that **26c** is the product of the *cis* ring opening. The NOEs seen in the NOESY spectrum of **26c** recorded in CDCl_3 at −25 °C support this conclusion: H3' and H5' display the NOE expected for 1,3-diaxial protons, while H3 and H5 do not. Similarly, **26a,b** display the NOEs between H3 and H5 and between H3' and H5'. The NOESY spectrum of **26a** indicates that the solution conformation is very similar to that observed in the solid state (Figure 5).

NOEs between H2 and H8', H3 and H8', and H2' and H2'' demonstrate that of all the possible conformations arising from rotation about the C3–O–C4' bond, **26a** adopts one in which C9' is close to C2. This is also confirmed by the NOEs of comparable size between H2 and H3 and between H2 and H4' and by a larger NOE of H4' with H2 than with H4. A larger NOE of the OH with H2 than with H2' indicates that the OH is oriented toward the tosyl group, but a small value for the temperature coefficient of the OH chemical shift suggests lack of hydrogen bonding. A coupling constant of 7.6 Hz for the NH, together with larger NOEs to H3 and H5 than to H4, indicates that the NH is antiperiplanar to H4. The phenyl group prefers a position on the same side of the molecule as C7, as suggested by NOEs between H2'' and H7.

The NOESY spectrum of **26b**, in CDCl_3 at −15 °C, displays an NOE between H2 and H4', which indicates that of all the conformations arising from rotation about the C3–O–C4' bond, **26b** adopts the one in which the OH and the NH are *anti*. NOEs of similar magnitude of H2 and H2' with H3 and H3' suggest

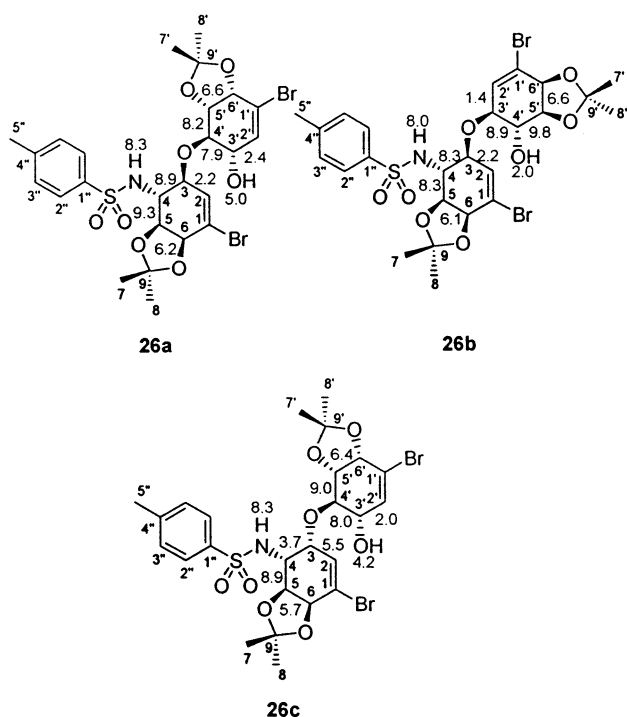


Figure 4. Position numbering and vicinal coupling constants (in Hz) for compounds 26a–c.

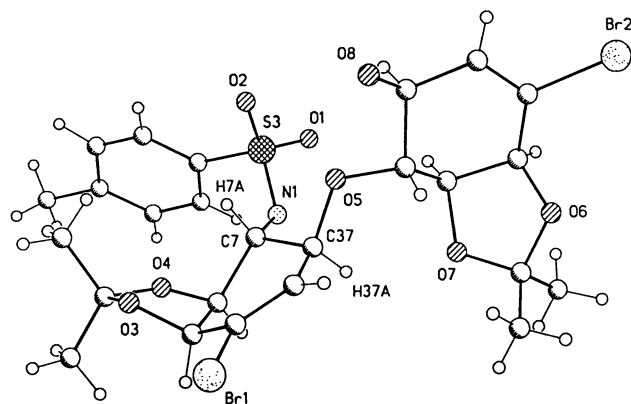


Figure 5. Crystal structure of dimer 26a as determined by X-ray diffraction.

that the bridge C3–O–C3' is twisted as to bring H3' closer to H2. Proton H2'' displays NOEs with H2', H4', and H7', which confirm that the tosyl group is *anti* to the OH with respect to the C3–O–C3' junction and on the same side of the cyclohexene ring C1'–C6' as H3'. The OH displays a vicinal coupling constant of 2.0 Hz and the only NOE with H4'; therefore it is most likely in one of the two gauche positions to this one. The NH has a vicinal coupling of 8.0 Hz and NOEs with H3, H4, and H5, consistent with the NH being antiperiplanar to H4. The temperature coefficients of the chemical shifts are smaller in 26b than in 26c. The protons experiencing larger values are H3, H2', and H4'; most likely the variation of the chemical shifts with the temperature is due to changes in the angle H3–C3–O–C3'–H3'. The hydroxyl proton has a small temperature coefficient, and most likely is not involved in any hydrogen bonding.

The exchangeable protons, NH and OH, display significant differences in chemical shifts and, most importantly, in the temperature coefficients of the chemical shifts between compounds 26c and 26b. Large negative temperature coefficients

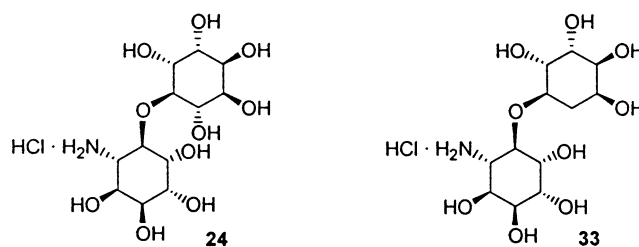


Figure 6. Comparison of the structures of 24 and 33.

indicate that in 26c both of the exchangeable protons are involved in hydrogen bonding. The solvent, CDCl₃, is not a hydrogen bond acceptor; therefore the hydrogen bonds have to be intramolecular, and of all the conformations arising from rotation about the C3–O–C4' bond, 26c has to adopt at low temperature the one in which the OH and the NH are *syn*. The NOESY spectrum of 26c at –25 °C displays the NOEs expected for such a conformation, i.e., H2–H7', H2–H5', OH–NH, H5–OH, NH–H3', and OH–H2''.

The NH is antiperiplanar to H4 ($J_{\text{NH-H4}} = 8.0$ Hz) and forms a hydrogen bond to the oxygen in the hydroxyl group, across the eight-member ring H···O–C3'–C4'–O–C3–C4–N, a picture confirmed by five large NOEs of the NH with OH, H4', H3, H4, and H5. Large NOEs of H7' with H2 and H3 agree with this hydrogen bonding, but only for the structure in which the substituents in positions 3 and 4 are *cis*. The OH proton displays a coupling of 4.2 Hz with H3' and NOEs with H2', H3', and H5; its most likely location is intercalated between C3'–H3' and C3'–C2. The coupling constants of the OH and NH do not vary significantly with temperature, indicating that the formation of the hydrogen bond produces only a small change in the orientation of these protons relative to their vicinal partners. The NOEs of H2'' with H3, H4, and H4' and the NOE of H3'' with H7' all demonstrate that the tosyl moiety is on the same side of the eight-member ring H···O–C3'–C4'–O–C3–C4–N as H4'. The protons having a large positive temperature coefficient of the chemical shifts, H3, H4, H4', and H7', are in the same region of space, which probably is the shielding region of the tosyl ring in the most stable conformation. Large temperature coefficients for the chemical shifts of H7 (negative) and H7' (positive) are more consistent with reorientation of the tolyl group upon the formation of a hydrogen bond between the OH hydrogen and an oxygen in the sulfonic moiety than with rotation about the C3–O–C4' bond upon the formation of the NH···O bond.

Calcium Binding Affinity Study

Our earlier report on the Ca²⁺ sequestering properties associated with amino diinositol 33¹⁴ prompted us to investigate the Ca²⁺ binding potential of all three oligomers, but especially 24, as it is configurationally identical to 32 except for one extra hydroxyl group. The binding affinity toward Ca²⁺ was studied for compounds 16, 17, 24, and 33 by monitoring the change in chemical shifts of the CH protons in deuterated water, upon titration with a D₂O solution of known ratio of CaCl₂ and acetic acid. The acetic acid was used to calculate the Ca²⁺/inositol ratio from the proton spectra. A plot of chemical shifts versus concentration showed a small variation of the chemical shifts (less than 0.03 ppm for a ratio Ca²⁺/inositol of 5) for compounds 16, 24, and 33. The change in the chemical shifts during titration of CH's 1–6 in these compounds also paralleled the temperature

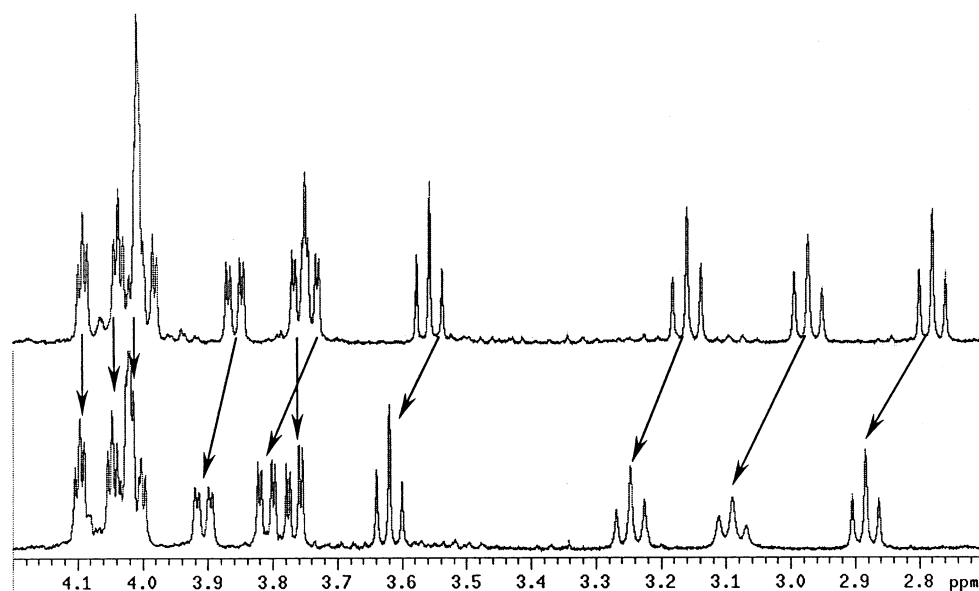


Figure 7. Calcium interaction studies of dimer **17**. Top spectrum is without Ca^{2+} , bottom one contains excess calcium ions.

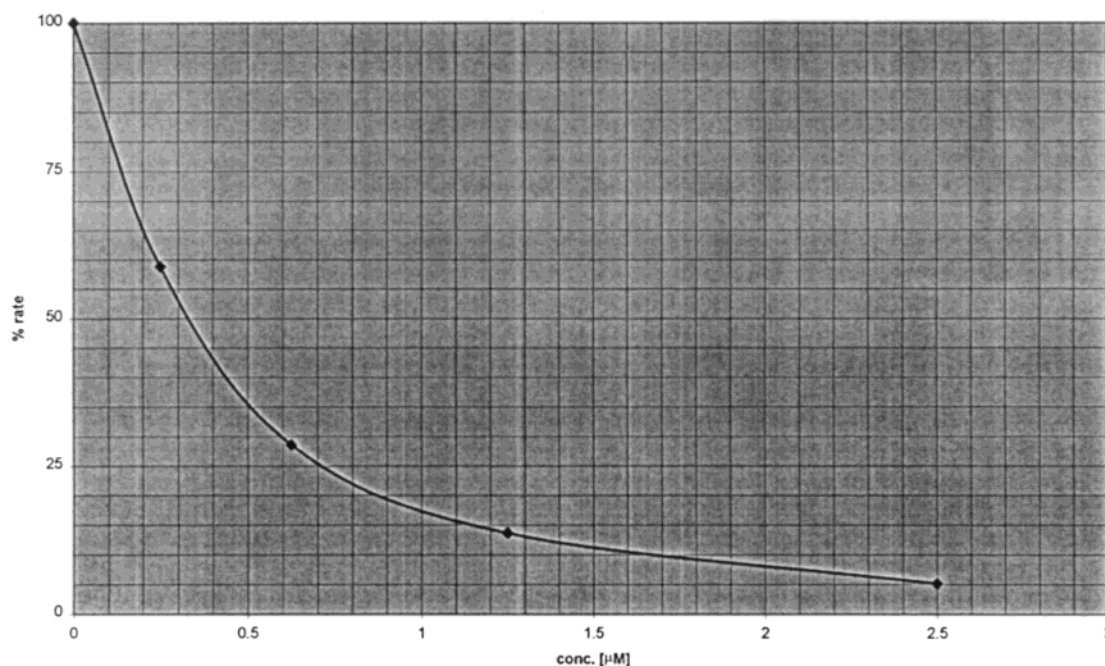


Figure 8. Inhibition of α -mannosidase by DIM (**31**).

coefficients of the corresponding OH's; therefore they merely reflect the change in the ionic strength of the solution and no Ca^{2+} binding occurs. In the case of compound **17**, a net change in chemical shift (0.1 to 0.2 ppm) is observed for what would be the protons nearest the nitrogen in the molecule, namely, protons in positions 3 and 4, which were identified by their two large couplings, signifying an axial proton with two axial neighbors. On the other hand, the protons assigned on the "periphery" of the molecule barely shift at all. This is clearly indicative of the molecule binding with calcium.

Glycosidase Inhibition Studies

For the evaluation of the glycosidase inhibition properties of inositol dimers, we first utilized the conventional assay.¹⁹ However, the screening of all compounds toward several

enzymes was very labor intensive, especially since we encountered problems with the reproducibility of our data using this protocol. To ensure a faster and less error-prone inhibition evaluation, we set our focus to modifying the current protocol to allow for a more rapid screening. (For a more detailed description see the Experimental Section.) All compounds were screened against the corresponding enzymes at or close to their optimum pH value, and the liberated *p*-nitrophenolate was monitored at 400 nm without a basic quench. We used a multicell spectrometer, which allowed the monitoring of the

(19) For examples see: (a) Saul, R.; Molyneux, R. J.; Elbein, A. D. *Arch. Biochem. Biophys.* **1984**, 230, 668–675. (b) Fleet, G. W. J.; Smith, P. W.; Evans, S. V.; Fellows, L. E. *J. Chem. Soc., Chem. Commun.* **1984**, 1240–1241. (c) Dale, M. P.; Ensley, H. E.; Kern, K.; Sastry, K. A. R.; Byers, L. D. *Biochemistry* **1985**, 24, 3530–3539. (d) Daniels, L. B.; Coyle, P. J.; Chiao, Y.-B.; Glew, R. H.; Labow, R. S. *J. Biol. Chem.* **1981**, 256, 3004–3013.

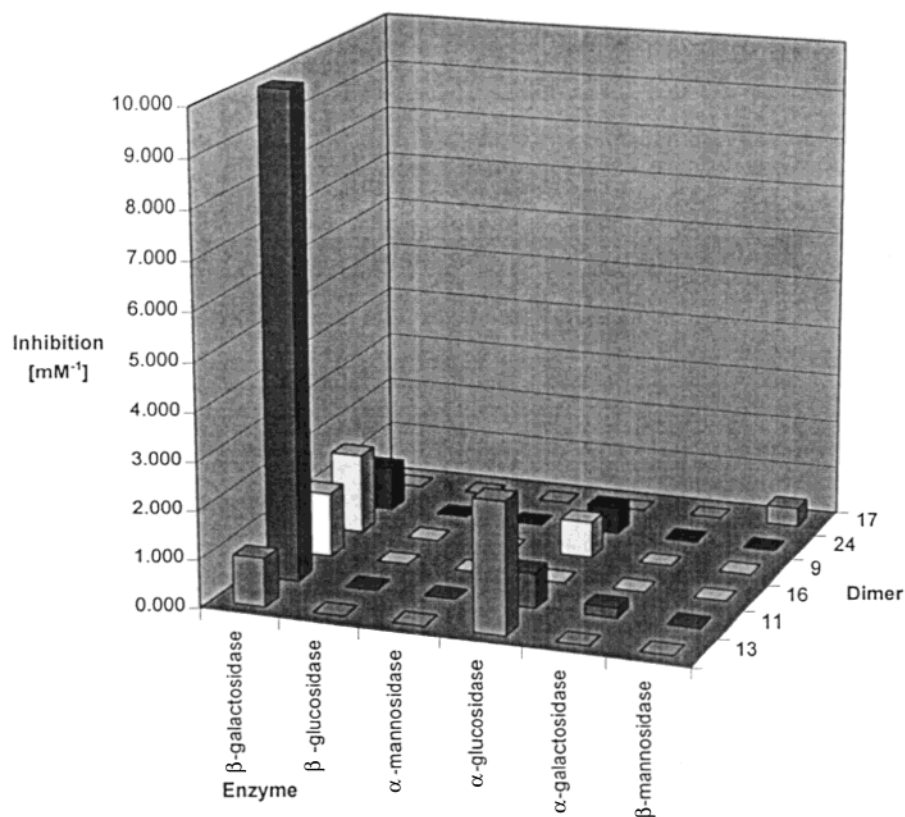


Figure 9. Glycosidase inhibition of inositol oligomers.

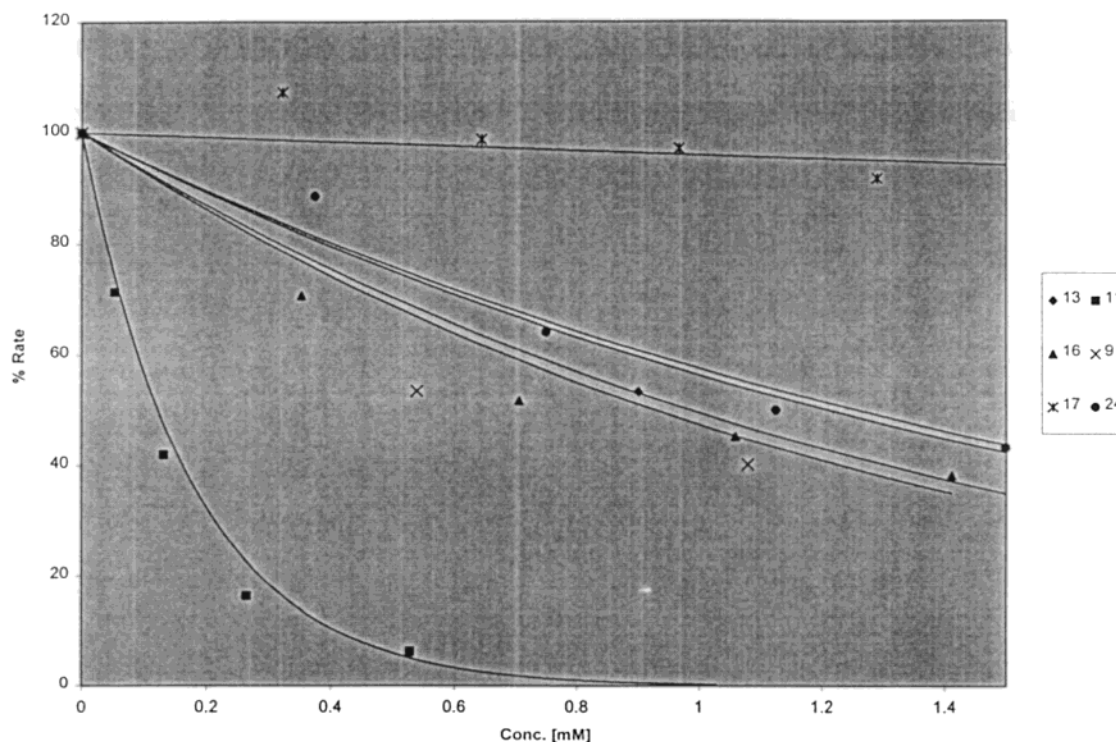


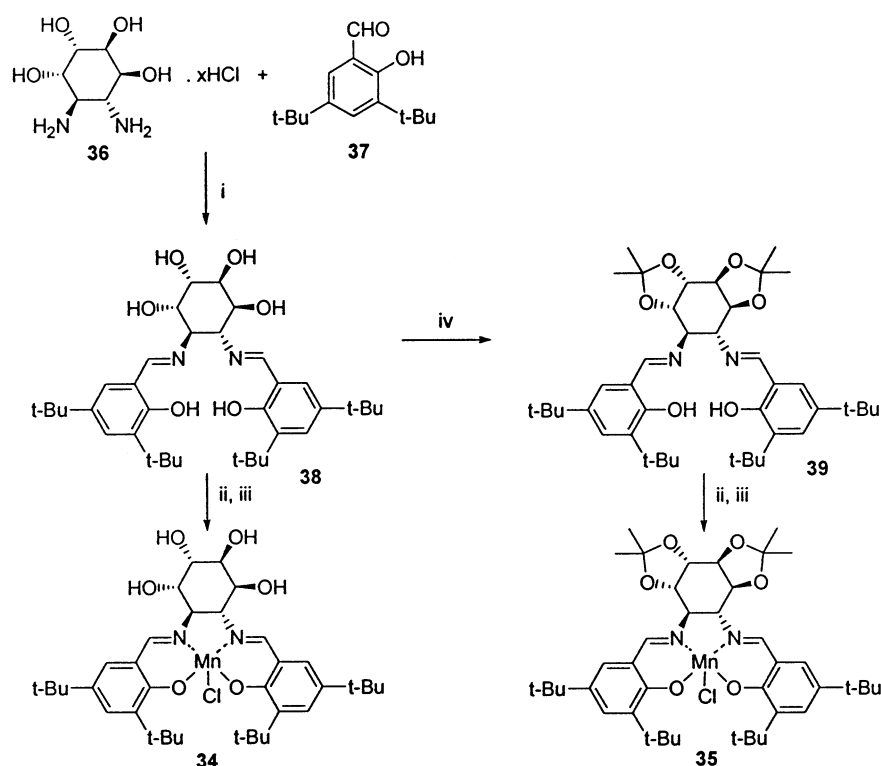
Figure 10. Inhibition of β -galactosidase.

enzymatic reaction at different inhibitor concentrations over a period of time (usually 20 min). For active compounds we observed a decrease of the initial rate with increasing inhibitor concentration. When plotting the reaction rates (normalized to the initial rate = 100%) against the inhibitor concentrations, inhibition curves were generated from which the corresponding

IC_{50} values could be obtained either graphically or by mathematical means.

Results and Discussion

To verify the reproducibility and accuracy of the assay, we compared the results of the new testing procedure with literature

Scheme 4^a

^a Reagents and conditions: (i) NaOMe, MS 3 Å, MeOH, EtOH, Δ; (ii) Mn(OAc)₂·4H₂O, EtOH, PhCH₃, Δ; (iii) air, then NaCl (sat.); (iv) DMP, H⁺.

Table 3. Glycosidase Inhibition of Inositol Oligomers

enzyme	inhibitor tested (IC ₅₀ , μM)					
	13	11	16	9	24	17
β-galactosidase	980	100	750	620	1120	n.I.
β-glucosidase	n.I. ^a	n.I.	n.I.	n.I.	n.I.	n.I.
α-mannosidase	n.I.	n.I.	n.I.	n.I.	n.I.	n.I.
α-glucosidase	370	1350	n.I.	1400	1750	n.I.
α-galactosidase	n.I.	n.I.	n.I.	n.I.	n.I.	n.I.
β-mannosidase	n.I.	n.I.	n.I.	n.I.	n.I.	n.I.

^a n.I. = less than 50% inhibition at an inhibitor concentration of 2000 μM.

values obtained by the traditional way. As a test substrate we chose 1,4-dideoxy-1,4-imino-D-mannitol (DIM) (**31**), a powerful inhibitor of α-mannosidase (Figure 8).

The literature reports an IC₅₀ value for DIM against α-mannosidase of 0.5 μM ([S] = 0.33 mM; pH = 4.5), whereas our assay produced a value of 0.35 μM ([S] = 2.5 mM; pH = 6.0).²⁰

By using the protocol described in this article, we obtained the inhibition data shown in Table 3 and Figure 9.

It was surprising to find that almost all oligomers were active against β-galactosidase, despite the fact that the peripheral substitution of these compounds does not correspond to the configuration of the natural D-galactose.

When comparing the structure of L-chiro-aminoinositol **13** and conduramine-F with β-D-galactose, it is evident that they do not possess the same hydroxylation pattern, except at three of the hydroxylated carbons. We may speculate that hydroxyl groups from both inositol rings as well as the acetamide oxygen might participate in the binding to the enzyme, a speculation

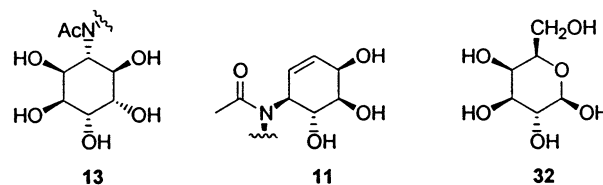


Figure 11. Comparison of the configuration of **13**, **11**, and β-D-galactose (**32**).

that will be confirmed or rejected when all monomeric units of **13** and **11** as well as the corresponding trimeric compounds are subjected to the same inhibition studies.

Inositol-Based Salen Complexes. During the synthesis of diamino derivative **19** we discovered a surprisingly efficient procedure for the synthesis of *trans*-1,2-diaminotetrahydrocyclohexanes. A preliminary account of the TBAF-catalyzed opening of a tosylaziridine with toluenesulfonamide has been published,²¹ and an initial investigation of the role of this compound in the design of (potentially) water-soluble catalysts for Jacobsen epoxidation has been made.

Thus the salen catalysts **34** and **35** have been prepared as shown in Scheme 4.

Previously reported²¹ 3,4-diamino-3,4-dideoxy-L-chiro-inositol (**36**) was treated with aldehyde **37** and base to afford salen complex **38**.²² The latter could be converted to manganese complex **34** by modifying Jacobsen's procedure.²³ Compound **38** was protected to afford salen-type species **39**, which was converted to protected catalyst **35** by following the same protocol.

(21) Paul, B. J.; Hobbs, E.; Buccino, P.; Hudlicky, T. *Tetrahedron Lett.* **2001**, 42, 6433–6435.

(22) Belekou, Y.; Ikonov, N.; Moscalenko, M.; North, M.; Orlova, S.; Tararov, V.; Yashkina, L. *Tetrahedron: Asymmetry* **1996**, 7, 851–855.

(23) Larrow, J. F.; Jacobsen, E. N.; Gao, Y.; Hong, Y.; Nie, X.; Zepp, C. M. *J. Org. Chem.* **1994**, 59, 1939–1942.

(20) Because of the low equilibrium concentration of *p*-nitrophenolate at pH = 4.5, we were unable to perform the assay at this low pH.

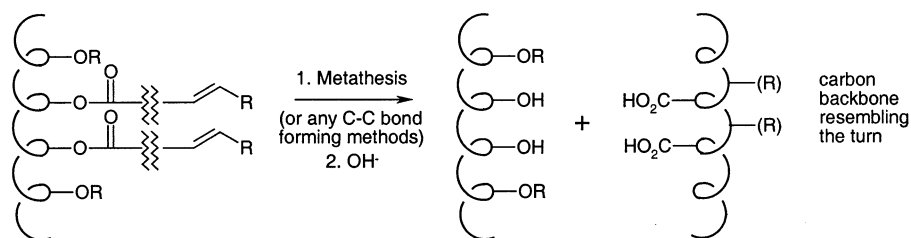


Figure 12. C–O to C–C connectivity translation.

Both catalysts **34** and **35** were compared to Jacobsen's original catalyst in the chiral epoxidation of styrene.^{24,25} Jacobsen's catalyst gave *S*-styrene oxide in an enantiomeric excess (ee) of almost 60% in this reaction at $-78\text{ }^{\circ}\text{C}$, whereas catalysts **34** and **35** afforded the *R*-configured product with an ee of 16% and 27%, respectively. We were also surprised to find that the four hydroxyl groups in catalyst **34** did not enhance its water solubility at all. Further endeavors in this field will focus on attaching polar groups (e.g., sulfates) on the alcohol moieties to increase the water solubility.

Conclusion

The *N*- and *O*-linked oligomers have been synthesized and subjected to glycosidase inhibition studies. For one of these compounds the precursory conduramine oligomers has been found more active, by an order of magnitude, than the corresponding fully hydroxylated analogue. This observation is in agreement with postulated models for the transition states in the hydrolysis of the glycosidic linkage: the cyclohexene motif of the conduritol (conduramine) resembles more closely the tetrahydropyranyl cation. Somewhat surprising was the finding that all compounds showed, albeit modest, activity against β -galactosidase. The configuration of its corresponding substrate is not reinforced in any of the tested compounds.

These preliminary results bode well for further investigation aimed at determining which structural units are responsible for increase or decrease of antiglycosidic activities.

The compounds themselves are also suited for a host of material or molecular recognition studies. Apart from the opportunities in catalyst design for compounds containing the *trans*-diamino cyclohexane motif, these structures may be used as templates for potential transfer of chirality from C–O bonds to C–C bonds by a number of processes such as free radical cascades, Heck-type cascades, or Grubb's metathesis bond formation of oxygen-tethered functional groups. One such possibility is outlined in Figure 12.

Further results in the investigation of chemistry, structure, biological activity, and catalytic or template roles of these oligomers will be reported in due course.

Experimental Section²⁶

General Procedure for the Inhibition Assays. The following buffers were used for the tests:

Sodium phosphate buffer (25mM) pH = 7.3 for β -galactosidase

Sodium phosphate buffer (25mM) pH = 6.8 for β -glucosidase, α -glucosidase

Sodium phosphate buffer (25mM) pH = 6.0 for α -mannosidase, α -galactosidase

Sodium phosphate buffer (25mM) pH = 5.5 for β -mannosidase

The inhibitor concentration was kept around 1 mg/mL. All tests were run at $37\text{ }^{\circ}\text{C}$, except for the α -mannosidase assay, which was performed at $25\text{ }^{\circ}\text{C}$. The substrate concentration was 5 mM except for the α - and β -mannosidase assay, where it was 2.5 mM. The enzyme concentration was adjusted to produce a slope of approximately 0.02–0.025 except for the β -mannosidase assay, where it was adjusted to give a slope of 0.005–0.01. The final volume (adjusted with the corresponding buffer) was 1000 μL in all cases.

To a solution of varying amounts of inhibitor (usually 0–400 μL) in the corresponding buffer solution was added 100 μL of the enzyme solution, except for one vial that was run as a blank to correct for the autohydrolysis of the substrate. All samples were preincubated at the corresponding temperature for 30 min, after which the reaction was started by addition of the substrate (400 μL). The absorption was then recorded over a period of 20 min by continually scanning all samples. The slopes obtained for the individual samples were then plotted against the inhibitor concentration to obtain the usual inhibition curves.

Aziridine–Alcohol Couplings: Typical Procedure. Borontrifluoride diethyl ether complex (24.7 μL , 250 μmol) in dry CH_2Cl_2 (15 mL) was added to a stirred solution of aziridine **18** (1.0 g; 2.50 mmol) and diol **25** (0.66 g; 2.50 mmol) at $-50\text{ }^{\circ}\text{C}$. The mixture was allowed to warm to $-10\text{ }^{\circ}\text{C}$ and stirred at that temperature for 20 min. A saturated solution of NaHCO_3 (20 mL) was added, and mixture was extracted with CH_2Cl_2 ($3 \times 30\text{ mL}$). The combined organic layers were dried (MgSO_4) and concentrated under reduced pressure. The products of the reaction (**26a–c**, **29**, **30**) were separated by flash chromatography (3:1 hexanes/ethyl acetate).

5,6-Bis[3,5-di-*tert*-butyl-2-hydroxybenzylidene]amino]cyclohexane-1,2,3,4-tetraol (38**).** To a solution of hydrochloride **36** (150 mg; 0.597 mmol), aldehyde **37** (308 mg; 1.3147 mmol), and crushed, activated molecular sieves (3 Å) in a 1:1 mixture of EtOH and MeOH (15 mL total) was added a 0.2 M solution of NaOMe in MeOH (12 mL), upon which the reaction mixture turned bright yellow. The solution was heated to reflux for 15 h and then allowed to cool to room temperature and concentrated in vacuo. The residue was redissolved in CH_2Cl_2 (20 mL) and filtered through a plug of silica and evaporated again. The residue was loaded on a flash-chromatography column and eluted with hexanes/ethyl acetate (1:1) to obtain **38** as a yellow foam (292 mg; 80%): $[\alpha]_{\text{D}}^{25} +206.6$ (*c* 0.60, CHCl_3); IR (film on NaCl) 3403, 2956, 2924, 2869, 1626, 913, 743 cm^{-1} ; ^1H NMR (CDCl_3 , 300 MHz) δ 8.35

(26) All nonaqueous reactions were performed using standard techniques for the exclusion of moisture and air. Methylene chloride and dioxane were distilled from calcium hydride, whereas ether and THF were dried over sodium/benzophenone. Thin-layer chromatography was performed on Silicycle plates and flash chromatography using Natland 200–400 mesh silica gel. Melting points were recorded on a Hoover Unimelt apparatus and are uncorrected. IR spectra were recorded on a Perkin-Elmer FT-IR or on a Perkin-Elmer Spectrum One FT-IR spectrometer. ^1H and ^{13}C NMR spectra were recorded on a Varian Gemini (300 MHz), a Varian VXR (300 MHz), a Mercury 300 (300 MHz), and an Inova 500 (500 MHz) instrument. All chemical shifts are referenced to TMS or residual undeuterated solvent. Optical rotations were measured on a Perkin-Elmer 341 instrument. All combustion analyses were performed by Atlantic Microlab, Norcross, GA. Mass spectra were recorded by the analytical division at the University of Florida, Gainesville.

(24) Palucki, M.; Pospisil, P. J.; Zhang, W.; Jacobsen, E. N. *J. Am. Chem. Soc.* **1994**, *116*, 9333–9334.

(25) Because of the easy availability of both enantiomers of styrene oxide, we chose styrene as a substrate, despite its moderate suitability as a substrate for the Jacobsen epoxidation.

(s, 2H), 7.33 (d, $J = 2.4$ Hz, 2H), 7.02 (d, $J = 2.4$ Hz, 2H), 4.20–4.432 (m, 4H), 3.64–3.74 (m, 2H), 1.40 (s, 18H), 1.22 (s, 18H); ^{13}C NMR (CDCl_3 , 75 MHz) δ 169.8, 158.1, 140.6, 136.8, 127.7, 126.8, 117.8, 71.9, 71.3, 70.2, 35.2, 34.3, 31.6, 29.6; HRMS calcd for $\text{C}_{36}\text{H}_{55}\text{N}_2\text{O}_6$ ($\text{M} + \text{H}$) $^+$ 611.4060, found 611.4062. Anal. Calcd for $\text{C}_{36}\text{H}_{54}\text{N}_2\text{O}_6$: C, 70.79; H, 8.91. Found: C, 70.25; H, 8.95.

5,6-Bis[(3,5-di-*tert*-butyl-2-hydroxybenzylidene)amino]cyclohexane-1,2,3,4-tetraol Manganese Complex (34). In a three-neck flask equipped with a reflux condenser was dissolved $\text{Mn}(\text{OAc})_2 \cdot 4\text{H}_2\text{O}$ (300 mg; 1.223 mmol) in EtOH (10 mL). The mixture was heated to reflux, after which a solution of ligand **47** (249 mg; 0.407 mmol) in toluene (10 mL) was added dropwise over a 5 min period. The mixture was allowed to reflux for 1.5 h, after which air was bubbled through the solution for 2 h. After that time, no more ligand **38** could be detected by TLC monitoring. Heating and air were discontinued, and the reaction mixture was quenched with brine (15 mL) and allowed to cool to room temperature. To the solution was added toluene (50 mL), the layers were separated, and the organic layer was washed with H_2O (2×20 mL) and brine (1×20 mL). After the solution was dried (Na_2SO_4) and concentrated, a brown residue was obtained, which was dissolved in CH_2Cl_2 (1 mL). To this solution was added heptane (10 mL), which caused precipitation after a few minutes. The crystals were removed by filtration, the mother liquor was evaporated, and the residue was subsequently dissolved again to obtain three more fractions. The combined precipitates were dried at high vacuum to obtain **34** as a brown solid (93 mg; 33%): $[\alpha]_D^{26} +830$ (c 0.013, CHCl_3); IR (film for $\text{C}_{36}\text{H}_{52}\text{MnN}_2\text{O}_6$ ($\text{M} - \text{Cl}$) $^+$ 663.3206, found 663.3225. Anal. Calcd for $\text{C}_{36}\text{H}_{52}\text{ClMnN}_2\text{O}_6 \cdot 1.5\text{H}_2\text{O}$: C, 59.54; H, 7.63; N, 3.86. Found: C, 59.34; H, 7.33; N, 3.74.

5,6-Bis[(2-hydroxy-3,5-dimethylbenzylidene)amino]cyclohexane-1,2,3,4-di-*O*-isopropylidene-1,2,3,4-tetraol (39). Ligand **38** (62 mg; 0.101 mmol) was dissolved in CH_2Cl_2 (5 mL) and DMP (200 μL). To this solution was added a spatula tip of *p*-TsOH, and the mixture was stirred at room temperature for 20 h. Additional DMP (200 μL) and *p*-TsOH (1 spatula tip) was added, and the mixture was allowed to stir an additional 10 h. After that, the reaction was quenched by adding excess solid Na_2CO_3 . The mixture was stirred for 5 min, filtered through a plug of Celite, washed with CH_2Cl_2 , and evaporated. The residue was purified by flash chromatography (gradient elution: starting with hexanes, ending with hexanes/ethyl acetate, 10:1) to obtain **39** as a yellow oil (52 mg; 73%): $[\alpha]_D^{26} +60.2$ (c 1.0, CHCl_3); IR (film on NaCl) 2957, 2871, 1738, 1630, 1598, 1468, 1441, 1382, 1370, 1362, 1273, 1250, 1060 cm^{-1} ; ^1H NMR (CDCl_3 , 300 MHz) δ 8.33 (s, 2H), 7.32 (d, $J = 1.9$ Hz, 2H), 7.03 (d, $J = 1.9$ Hz, 2H), 4.61 (d, $J = 5.2$ Hz, 2H), 4.48 (dd, $J = 7.1, 5.2$ Hz, 2H), 3.44 (dd, $J = 5.2, 2.1$ Hz, 2H), 1.58 (s, 6H), 1.40 (s, 6H), 1.39 (s, 18H), 1.25 (s, 18H); ^{13}C NMR (CDCl_3 , 75 MHz) δ 168.7, 158.2, 140.3, 136.6, 132.7, 127.5, 126.7,

117.9, 109.3, 77.7, 75.5, 71.2, 35.1, 34.2, 31.6, 29.6, 28.3, 25.8; HRMS calcd for $\text{C}_{42}\text{H}_{63}\text{N}_2\text{O}_6$ ($\text{M} + \text{H}$) $^+$ 691.4686, found 691.4683. Anal. Calcd for $\text{C}_{42}\text{H}_{62}\text{N}_2\text{O}_6 \cdot 0.5\text{H}_2\text{O}$: C, 72.07; H, 9.07; N, 4.00. Found: C, 71.91; H, 8.98; N, 3.79.

5,6-Bis[(2-hydroxy-3,5-dimethylbenzylidene)amino]cyclohexane-1,2,3,4-di-*O*-isopropylidene-1,2,3,4-tetraol Manganese Complex (35). In a two-neck flask equipped with a reflux condenser was dissolved $\text{Mn}(\text{OAc})_2 \cdot 4\text{H}_2\text{O}$ (64 mg; 0.260 mmol) in EtOH (3 mL). The mixture was heated to reflux, after which a solution of ligand **549** (60 mg; 0.868 mmol) in toluene (3 mL) was added dropwise over a 5 min period. The mixture was allowed to reflux for 45 min, after which air was bubbled through the solution for 5 h. After that time, no more ligand **39** could be detected by TLC monitoring. Heating and air were discontinued, and the reaction mixture was quenched with brine (15 mL) and allowed to cool to room temperature. To the solution was added toluene (15 mL), the layers were separated, and the organic layer was washed with H_2O (2×5 mL) and brine (1×5 mL). After the solution was dried (Na_2SO_4) and concentrated, a brown residue was obtained, which was dissolved in CH_2Cl_2 (1 mL). To this solution was added heptane (10 mL), which caused precipitation after a few minutes. The crystals were removed by filtration, the mother liquor was evaporated, and the residue was subsequently dissolved again to obtain three more fractions. The combined precipitates were dried at high vacuum to obtain crude **35** as a brown solid (21 mg; 31%). No further purification of **35** was performed: $[\alpha]_D^{30} +141.5$ (c 0.050, CHCl_3); IR (film on NaCl) 3435, 1644, 1616, 1532, 1260 cm^{-1} ; HRMS calcd for $\text{C}_{42}\text{H}_{60}\text{MnN}_2\text{O}_6$ ($\text{M} - \text{Cl}$) $^+$ 743.3832, found 743.3826. Anal. Calcd for $\text{C}_{42}\text{H}_{60}\text{ClMnN}_2\text{O}_6$: C, 64.73; H, 7.76; N, 3.59. Found: C, 43.69; H, 5.52; N, 1.98.

Acknowledgment. The authors are grateful to the following agencies for generous financial support: The National Science Foundation (CHE-9615112, CHE-9910412), the U.S. Environmental Protection Agency (R- 826113), TDC Research Foundation, Inc., TDC Research, Inc., the McKnight Foundation (Fellowship for J.W.), and the University of Florida (fellowship for TM). The authors would like to thank Prof. Jon Stewart for helpful discussions and for the access to his spectrometer. Skillful assistance of Pablo Buccino and Elizabeth Hobbs in the preparation of starting materials is appreciated.

Supporting Information Available: Crystallographic data (CIF). This material is available free of charge via the Internet at <http://pubs.acs.org>.

JA0205378